ChemComm

COMMUNICATION

View Article Online
View Journal | View Issue

Cite this: *Chem. Commun.*, 2022, 58, 10727

Received 7th January 2022,
Accepted 8th August 2022

DOI: 10.1039/d2cc00118g

rsc.li/chemcomm

An endoplasmic reticulum targeting green fluorescent protein chromophore-based probe for the detection of viscosity†

Xiaoqin Wei, ‡[a] Yiming Zhu,‡[a] Xiang Yu,[a] Lei Cai,[a] Nanan Ruan,[a] Luling Wu, *[ab] Nengqin Jia,[a] Tony D. James *[bc] and Chusen Huang *[a]

The occurrence of endoplasmic reticulum (ER) stress is the main cause of a variety of biological processes that are closely related to numerous diseases. The homeostasis of the ER microenvironment can be disrupted under ER stress. In this research, by linking a pentafluorophenyl to the green fluorescent protein chromophore, we have developed a new ER-targeting fluorescent probe (GE-Y) for measuring changes of intracellular ER viscosity caused by ER stress. Importantly, an increase in ER viscosity was observed using GE-Y in cells undergoing autophagy. As such, our research provides an ideal tool for studying ER stress and autophagy.

Green fluorescent protein (GFP), a luminescent protein discovered from the jellyfish Aequorea victoria in 1962, is widely used in protein localization, gene transcription regulation and cytoskeleton research.[1–3] The core chromophore of GFP, *p*-hydroxybenzylidene imidazolidinone (HBDI), is non-fluorescent in solution due to the rotation of the excited state of the double bond between the phenyl and imidazolidinone.[4] In order to expand the applications of the GFP chromophore, two strategies have been developed: (1) restriction of the free rotation through formation of host–guest complexes, such as interaction with β-cyclodextrin,[5] MOFs,[6] and host proteins,[7] (2) enhancement of the intrinsic torsional barrier for the chromophore by the introduction of substituents.[8,9] Significantly, the GFP chromophore has not been extensively explored for the design of fluorescent probes suitable for the mapping of cellular viscosity until recently when our group reported on a HBDI-based fluorescent probe to detect the viscosity of lysosomes in live cells.[10,11]

The endoplasmic reticulum (ER) is a significant multifunctional organelle in eukaryotic cells and is responsible for the synthesis and metabolism of lipids and steroids, maintenance of Ca^{2+} homeostasis, protein synthesis, folding and post-translational modification.[12] However, some external factors such as infection,[13] hypoxia,[14] and inflammation[15] can disrupt protein folding. Consequently, the accumulation of unfolded or misfolded proteins within the ER may influence the normal physiological functions of the organelle, which can trigger an imbalance in homeostasis within the ER and as such induce ER stress. ER stress plays a key role in protecting cells by initiating the unfolded protein response to eliminate misfolded proteins. While ER stress can also induce autophagy when it persists for a long time. Studies have shown that the coexistence of ER stress and autophagy are closely related to cardiovascular disease, senile dementia, diabetes, and cancer.[16,17]

As an important intracellular parameter, intracellular viscosity plays an important role in material transfer, information transmission and the interaction of biological macromolecules.[18] It has been reported that during ER stress, protein accumulation in the ER cavity will inevitably lead to changes of viscosity. To date, changes of viscosity during ER stress remain poorly understood, which is the result of a lack of tools for the measurement of ER viscosity *in situ*.

Traditional instruments for measuring viscosity include the rotational,[19] falling ball[20] and capillary[21] viscometers which are not suitable for intracellular measurements. However, over the past few years, microscopic viscosity detection technologies including optical tweezers,[22] fluorescence imaging,[23] and rotational Brownian motion of microbeads[24] have been developed. Among these methods, fluorescence molecular imaging, which exhibits high selectivity, is noninvasive, and facilitates direct visualization and *in situ* detection, has become a powerful tool and attracted significant attention. To date, researchers have developed a variety of small-molecule organic rotors for monitoring the viscosity of cells.[23,25] In addition, subcellular organelle targeting viscosity-responsive probes

[a] *The Education Ministry Key Laboratory of Resource Chemistry, Shanghai Key Laboratory of Rare Earth Functional Materials, and Shanghai Frontiers Science Research Base of Biomimetic Catalysis, Department of Chemistry, Shanghai Normal University, 100 Guilin Road, Shanghai 200234, China. E-mail: huangcs@shnu.edu.cn*
[b] *Department of Chemistry, University of Bath, BA2 7AY, UK. E-mail: wllcyl@126.com, T.D.James@bath.ac.uk*
[c] *School of Chemistry and Chemical Engineering, Henan Normal University, Xinxiang 453007, China*

† Electronic supplementary information (ESI) available. See DOI: https://doi.org/10.1039/d2cc00118g

‡ Equal contribution.

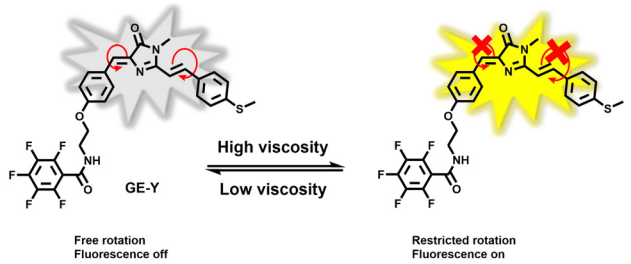

Scheme 1 Design of probe **GE-Y** for monitoring the viscosity within the endoplasmic reticulum.

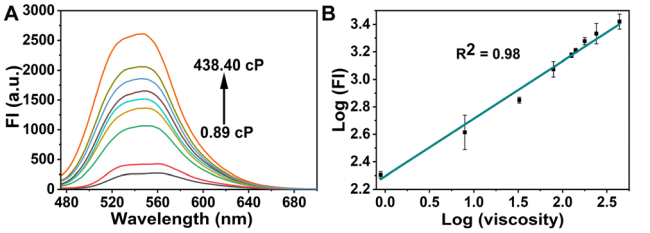

Fig. 1 (A) Fluorescence spectra of **GE-Y** (10 μM) in PBS/glycerin binary solutions of increased viscosities (from 0.89 cP to 438.4 cP). The solution was prepared by varying the ratio of PBS buffer (10 mM, pH 7.4) and glycerin. (B) Linear relationship between the logarithm of fluorescence intensity (log (FI)) (λ_{em} = 550 nm) and logarithm of viscosity (log (viscosity)) from panel (A). λ_{ex} = 430 nm, λ_{em} = 550 nm. Slit widths ex = 10 nm and em = 10 nm; temperature, 25 °C.

have also been reported. However, most subcellular organelle targeting probes have focused on viscosity detection in the mitochondria[26–28] and lysosomes,[29–32] while few systems have been developed for monitoring the viscosity of the ER.[33–37] Fluorescent probes that have been developed for ER viscosity have been based on BODIPY,[33,34,37] hemicyanine[36] and iridium complex[35] molecular rotors (Scheme S2, ESI†).

In this research, we have developed a fluorescent probe **GE-Y** for monitoring changes of viscosity in the ER of living cells. The GFP chromophore HBDI was used as the fluorophore. A methyl phenyl sulfide was connected to the imidazolinone ring through an ethylenic bond to enlarge the conjugated π-system of the probe for the purpose of red-shifting the emission wavelength (Scheme 1). In addition, pentafluorobenzene was attached to the hydroxyl of the aryl group and serves as a targeting group for the ER. In a low-viscosity environment, free rotation of the benzyl group and the C=C double bonds between the imidazolinone and the phenylthio group cause the energy of the excited state to be lost in a non-radiative manner, resulting in a low fluorescence quantum yield of the probe. However, in an environment of high viscosity, free rotation is inhibited, and the fluorescence emission of the probe is significantly enhanced.

To explore the optical properties of the probe **GE-Y**, the UV-Vis absorption and fluorescence emission spectra in PBS buffer (10 mM, pH 7.4) and glycerin were evaluated. As shown in Fig. S1A (ESI†), the absorption peak of **GE-Y** is located at 430 nm both in PBS buffer and in glycerin. However, the intensity of absorption in glycerin is higher than that in PBS buffer. **GE-Y** exhibits negligible fluorescence emission in PBS buffer, which can be attributed to the low viscosity of PBS buffer. In contrast, in glycerin with high viscosity a dramatic fluorescence off–on response is observed (Fig. S1B, ESI†). The emission enhancement can be attributed to restricted rotation in the high viscosity system. In addition, we investigated the fluorescence response of **GE-Y** towards increasing viscosity using a binary system of PBS/glycerin of different viscosity. As shown in Fig. 1A, the fluorescence intensity increases gradually with an increase of viscosity, with an approximate 10-fold enhancement in fluorescence intensity being observed on an increase of viscosity from 0.89 cP to 438.4 cP, suggesting that **GE-Y** is particularly sensitive towards changes of viscosity. In accordance with the Förster and Hoffmann equation,[38] there is a good linear relationship between log (FI) and log (viscosity) at 550 nm (R^2 = 0.98) (Fig. 1B). Moreover, we evaluated the fluorescence quantum yield (Φ) of the probe in low viscosity (0.89 cP) and high viscosity (438.4 cP) environments, respectively. As shown in Fig. S2 and Table S2 (ESI†), the fluorescence quantum yield of the probe in the high viscosity environment (Φ = 0.13) was significantly increased when compared with the low viscosity (Φ = 0.01) environment. All these results indicate that **GE-Y** has the potential to be used as a sensitive fluorescent probe for viscosity detection.

To further evaluate the enhancement in fluorescence intensity by variations of solvent polarity, the fluorescence emission spectra in different solvents were also evaluated. As expected, **GE-Y** shows very strong fluorescence signals in glycerin compared to in other solvents (Fig. S3, ESI†). This result suggested that polarity exhibits a negligible effect on the fluorescence off–on response of **GE-Y**.

Subsequently, we measured the effect of pH on the performance of **GE-Y** in high-viscosity (240.70 cP) and low-viscosity (7.90 cP) PBS/glycerin systems. As shown in Fig. S4 (ESI†), there are minimal changes of the maximum emission intensity of **GE-Y** when the pH changes from 3.32 to 10.98, illustrating that changes in pH hardly influence the probe.

Next, we evaluated the selectivity of **GE-Y** in the presence of various common species that may exist in living organisms. Therefore, common interfering species including cations (Fe^{2+}, Fe^{3+}, Mn^{2+}, Ca^{2+}, K^+, Zn^{2+}, Na^+), anions (Br^-, NO_2^-, SO_4^{2-}, ClO^-, $ONOO^-$), and amino acids (homocysteine, cysteine, glutathione, glycine, L-threonine, L-arginine) were added to **GE-Y** in PBS (10 mM, pH 7.4), respectively, and none of the species induce significant fluorescence changes (Fig. S5, ESI†). We then repeated the interference assay in a high viscosity environment. As shown in Fig. S6 (ESI†), the fluorescence intensity of 10 μM **GE-Y** in a solution with viscosity value at 126.80 cP did not change significantly after the addition of various competing reagents (including 1 mM for ClO^-, $ONOO^-$ and amino acids, 100 mM for other cations and anions). Thus, **GE-Y** exhibits high selectivity towards viscosity, even in the presence of high concentrations of other biological species. In addition, **GE-Y** was stable in the presence of ROS species including ClO^- and $ONOO^-$. All the results confirm that **GE-Y** is suitable for measuring the viscosity in complex biological systems.

Having established a fluorescence method for the sensitive and selective detection of viscosity in solution, we then explored the use of **GE-Y** for tracing the viscosity changes of

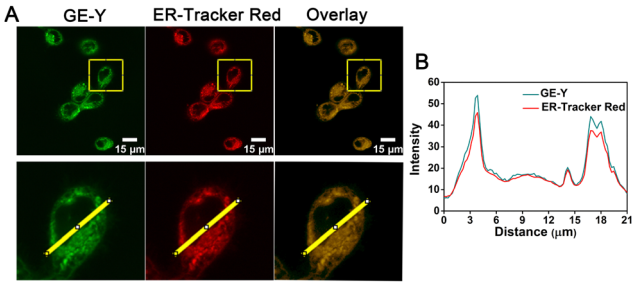

Fig. 2 (A) Colocalization cell images of **GE-Y**. MCF-7 cells co-stained with 10 μM **GE-Y** and 1 μM ER-Tracker Red for 20 min. Green channel (λ_{ex} = 488 nm, λ_{em} = 520–560 nm, voltage of PMT: 550 V): **GE-Y**. Red channel (λ_{ex} = 561 nm, λ_{em} = 600–640 nm): ER-tracker Red. Top row: The whole images; bottom row: enlarged regions of interest (ROI) of the top row. Scale bar is 15 μm. (B) ImageJ software was used for the fluorescence intensity profile of bottom row ROI analysis. The red line was from ER-Tracker Red, and the green line was from **GE-Y**.

live cells. Initially, a standard MTT assay was conducted to assess the toxicity of different concentrations of **GE-Y** (0 μM, 4 μM, 8 μM, 12 μM, 16 μM, and 20 μM, respectively). From Fig. S7 (ESI†) the cell survival rate remains above 90% when the cells were incubated with probe **GE-Y** for 6 h. In addition, when the concentration of **GE-Y** is lower than 16 μM, there is no effect on the viability of the cells even if the incubation time is extended to 12 h. Therefore, we selected 10 μM **GE-Y** for cell imaging, for extended monitoring of viscosity changes in live cells. We then performed a colocalization experiment to verify the ER targeting capability of **GE-Y**. MCF-7 cells were co-stained with **GE-Y** (10 μM) and commercially available ER-Tracker Red (1 μM) for 20 min. The results of the colocalization experiment using a confocal laser microscope are shown in Fig. 2. The green fluorescence of **GE-Y** and the red fluorescence of ER-Tracker Red are significantly overlapped. (The Pearson's colocalization coefficient was 0.95.) To demonstrate the superior ER-targeting capability of **GE-Y**, co-localization experiments were also performed using A549 cells, HeLa cells and CHO cells. As shown in Fig. S8 (ESI†), the green and red channels overlapped well in all the cell lines, with Pearson's colocalization coefficients of 0.97 in A549 cells, 0.96 in HeLa cells and 0.98 in CHO cells, demonstrating that probe **GE-Y** is mainly located in the ER.

After verifying the high ER-targeting ability of **GE-Y** in live cells, we then used **GE-Y** to trace the viscosity changes under ER stress in living MCF-7 cells. Tunicamycin was used to increase the ER viscosity because it is an antibiotic that can inhibit *N*-glycosylation to cause an accumulation of unfolded proteins in the ER[39] and induce ER stress.[33] As shown in Fig. 3, the intracellular fluorescence increases gradually with an increase in incubation time (Fig. 3A). Specifically, the cells treated with tunicamycin for 90 min exhibited a remarkable fluorescence enhancement compared to the cells treated with tunicamycin for 0 min. Furthermore, a semi-quantitative analysis of the intracellular fluorescence intensity using ImageJ software indicated a 3.5-fold enhancement after the cells were treated with tunicamycin for 90 minutes. The enhancement in the intracellular fluorescence could be ascribed to an increased ER viscosity that was induced by the addition of tunicamycin. As such, **GE-Y** can be used as a visualization tool for measuring changes of intracellular viscosity.

Autophagy and ER stress are independent biological processes. However, a growing amount of research has indicated that there is a close relationship between ER stress and autophagy.[40,41] As such, ER stress can induce autophagy and in turn, the elevated ER stress will activate autophagy to counteract the high stress on the ER by degrading accumulated misfolded proteins. However, the detailed biological interplay of mechanisms associated with ER stress and autophagy remains unclear.[42] Therefore, we used probe **GE-Y** to monitor viscosity fluctuations in the ER during autophagy to evaluate the relationship between the two processes. There are two common methods for the induction of autophagy, one is

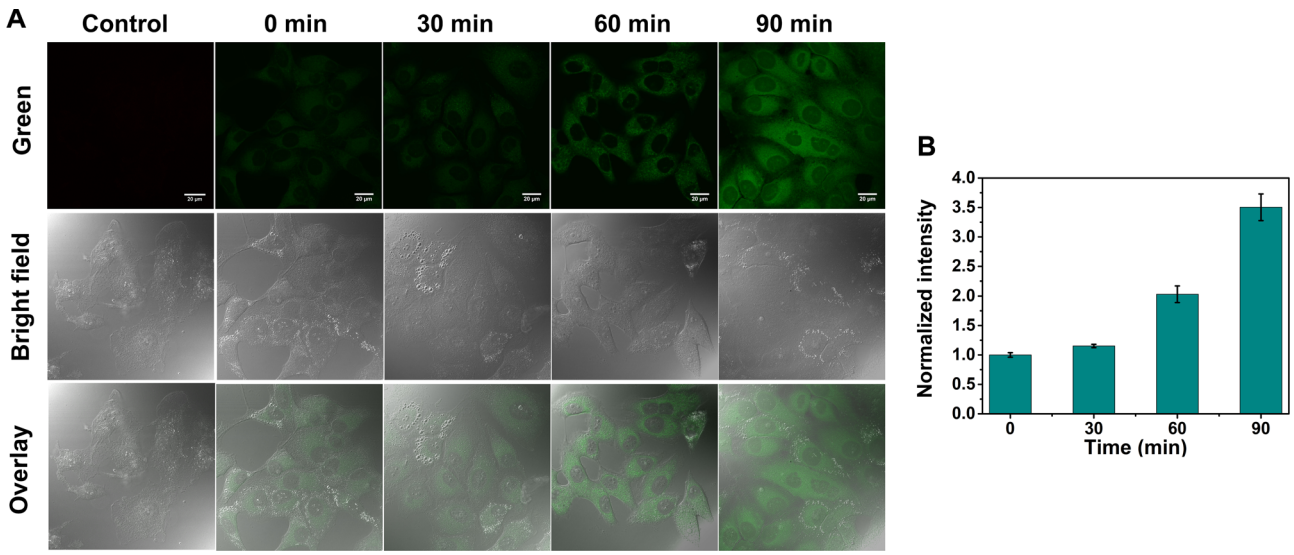

Fig. 3 (A) Confocal microscopic images of live MCF-7 cells treated with tunicamycin (40 μg mL^{-1}) for 0 min, 10 min, 40 min, and 70 min, respectively, and then stained with 10 μM **GE-Y** for 20 min (λ_{ex} = 488 nm, λ_{em} = 520–560 nm, voltage of PMT: 450 V). The control panel is the cells that were not treated with **GE-Y**. Scale bar, 20 μm. (B) Semi-quantitative analysis of averaged fluorescence intensity of (A). error bar represents s.d.

starvation and the other is drug induced.[43] As such Hanks' Balanced Salt Solution (HBSS) was used to induce autophagy of the cells through the starvation method.[44] Protein light chain 3(LC3), which includes two forms LC3-I and LC3-II, is a biomarker of autophagy.[45] When autophagy occurs, the LC3 precursor is cleaved to form LC3-I. Subsequently, LC3-I transforms to membrane-bound LC3-II.[46] As such an elevated ratio of LC3-II to LC3-I indicates enhanced autophagic activity.[47,48] We monitored the ratio of LC3-II/LC3-I by western blot to ensure autophagy occurred in the experimental group (Fig. S9 and Table S3, ESI†). From Fig. S10 (ESI†), the fluorescence intensity of cells undergoing autophagy was enhanced remarkably over the control cells, clearly indicating the higher viscosity of the ER during autophagy. These results indicated that both ER stress and autophagy can lead to an increase in ER viscosity, confirming that ER stress is closely related to autophagy. As such **GE-Y** exhibits great potential for use in exploring the detailed mechanisms between cellular autophagy and ER stress.

In summary, we have developed a fluorescent probe (**GE-Y**) based on the GFP-chromophore (HBDI) for monitoring changes in ER viscosity. **GE-Y** exhibited high selectivity and rapid response to viscosity changes in solution. In addition, **GE-Y** was able to monitor intracellular ER viscosity changes during stress through the time-dependent fluorescence signal readout. **GE-Y** was then used to monitor changes in ER viscosity during autophagy. The results indicated that autophagy could cause an increase in the viscosity of the ER, confirming the relationship between ER stress and autophagy. This research indicates that **GE-Y** is an effective tool for monitoring the viscosity of the ER, whilst also providing a powerful tool for monitoring ER stress during autophagy and related diseases.

The authors gratefully acknowledge the financial support from the National Natural Science Foundation of China (Grants 21672150 and 21302125), Shanghai Rising-Star Program (19QA1406400), and Shanghai Government (18DZ2254200). T. D. J. wishes to thank the Royal Society for a Wolfson Research Merit Award and the Open Research Fund of the School of Chemistry and Chemical Engineering, Henan Normal University for support (2020ZD01). L. W. wishes to thank the China Scholarship Council and the University of Bath for supporting his PhD in the United Kingdom.

Conflicts of interest

There are no conflicts to declare.

Notes and references

1 J. Lippincott-Schwartz and G. H. Patterson, *Science*, 2003, **300**, 87–91.
2 A. Miyawaki, *Annu. Rev. Biochem.*, 2011, **80**, 357–373.
3 D. C. Prasher, V. K. Eckenrode, W. W. Ward, F. G. Prendergast and M. J. Cormier, *Gene*, 1992, **111**, 229–233.
4 A. Acharya, A. M. Bogdanov, B. L. Grigorenko, K. B. Bravaya, A. V. Nemukhin, K. A. Lukyanov and A. I. Krylov, *Chem. Rev.*, 2017, **117**, 758–795.
5 S. Ge, H. Deng, Y. Su and X. Zhu, *RSC Adv.*, 2017, **7**, 17980–17987.
6 A. Singh, D. Samanta, M. Boro and T. K. Maji, *Chem. Commun.*, 2019, **55**, 2837–2840.
7 Y. Liu, C. H. Wolstenholme, G. C. Carter, H. Liu, H. Hu, L. S. Grainger, K. Miao, M. Fares, C. A. Hoelzel, H. P. Yennawar, G. Ning, M. Du, L. Bai, X. Li and X. Zhang, *J. Am. Chem. Soc.*, 2018, **140**, 7381–7384.
8 S. Chatterjee, K. Ahire and P. Karuso, *J. Am. Chem. Soc.*, 2020, **142**, 738–749.
9 M.-S. Tsai, S.-Y. Tsai, Y.-F. Huang, C.-L. Wang, S.-S. Sun and J.-S. Yang, *Chem. - Eur. J.*, 2020, **26**, 5942–5945.
10 X. Li, R. Zhao, Y. Wang and C. Huang, *J. Mater. Chem. B*, 2018, **6**, 6592–6598.
11 L. Cai, H. Li, X. Yu, L. Wu, X. Wei, T. D. James and C. Huang, *ACS Appl. Bio Mater.*, 2021, **4**, 2128–2134.
12 S. Sun, X. Tang, Y. Guo and J. Hu, *Curr. Opin. Cell Biol.*, 2021, **71**, 1–6.
13 A. C.-H. Chen, L. Burr and M. A. McGuckin, *Clin. Transl. Immunol.*, 2018, **7**, e1019.
14 M. Akman, D. C. Belisario, I. C. Salaroglio, J. Kopecka, M. Donadelli, E. De Smaele and C. Riganti, *J. Exp. Clin. Cancer Res.*, 2021, **40**, 28.
15 N. T. Sprenkle, S. G. Sims, C. L. Sánchez and G. P. Meares, *Mol. Neurodegener.*, 2017, **12**, 42.
16 K. Park, S. E. Lee, K.-O. Shin and Y. Uchida, *FEBS J.*, 2019, **286**, 413–425.
17 K. R. Bhattarai, M. Chaudhary, H.-R. Kim and H.-J. Chae, *Trends Cell Biol.*, 2020, **30**, 672–675.
18 J. Lippincott-Schwartz, E. Snapp and A. Kenworthy, *Nat. Rev. Mol. Cell Biol.*, 2001, **2**, 444–456.
19 C. S. Cardoso de Castro, D. M. d E. Santo Filho, J. R. R. Siqueira, A. P. F. Barbosa, C. R. d C. Rodrigues, M. L. Cabral, E. M. da Silva, F. d O. Baldner and J. M. G. Gouveia, *J. Pet. Sci. Eng.*, 2016, **138**, 292–297.
20 B. Calvignac, E. Rodier, J.-J. Letourneau, P. Vitoux, C. Aymonier and J. Fages, *J. Supercrit. Fluids*, 2010, **55**, 96–106.
21 E. Lee, B. Kim and S. Choi, *Sens. Actuators, A*, 2020, **313**, 112176.
22 A. Statsenko, W. Inami and Y. Kawata, *Opt. Commun.*, 2017, **402**, 9–13.
23 C. Ma, W. Sun, L. Xu, Y. Qian, J. Dai, G. Zhong, Y. Hou, J. Liu and B. Shen, *J. Mater. Chem. B*, 2020, **8**, 9642–9651.
24 C.-J. Chen, W.-L. Chen, P. H. Phong and H.-S. Chuang, *Sensors*, 2019, **19**, 1217.
25 F. Liu, Z. Yuan, X. Sui, C. Wang, M. Xu, W. Li and Y. Chen, *Chem. Commun.*, 2020, **56**, 8301–8304.
26 X. Mu, Y. Liu, S. Liu, Y. Sun, N. Lu, Y. Lu, W. Li, X. Zhou, B. Liu and Z. Li, *Sens. Actuators, B*, 2019, **298**, 126831.
27 X. Wang, L. Fan, S. Wang, Y. Zhang, F. Li, Q. Zan, W. Lu, S. Shuang and C. Dong, *Anal. Chem.*, 2021, **93**, 3241–3249.
28 J. Yin, M. Peng and W. Lin, *Anal. Chem.*, 2019, **91**, 8415–8421.
29 J. Cui, H. Nie, S. Zang, S. Su, M. Gao, J. Jing and X. Zhang, *Sens. Actuators, B*, 2021, **331**, 129432.
30 J. Park, B. Lim, N. K. Lee, J. H. Lee, K. Jang, S. W. Kang, S. Kim, I. Kim, H. Hwang and J. Lee, *Sens. Actuators, B*, 2020, **309**, 127764.
31 B. Shen, L. F. Wang, X. Zhi and Y. Qian, *Sens. Actuators, B*, 2020, **304**, 127271.
32 L. Wang, Y. Xiao, W. Tian and L. Deng, *J. Am. Chem. Soc.*, 2013, **135**, 2903–2906.
33 Z. Yang, Y. He, J. H. Lee, W.-S. Chae, W. X. Ren, J. H. Lee, C. Kang and J. S. Kim, *Chem. Commun.*, 2014, **50**, 11672–11675.
34 Y. He, J. Shin, W. Gong, P. Das, J. Qu, Z. Yang, W. Liu, C. Kang, J. Qu and J. S. Kim, *Chem. Commun.*, 2019, **55**, 2453–2456.
35 L. Hao, Y.-M. Zhong, C.-P. Tan and Z.-W. Mao, *Chem. Commun.*, 2021, **57**, 5040–5042.
36 Y. Zhou, Z. Liu, G. Qiao, B. Tang and P. Li, *Chin. Chem. Lett.*, 2021, **32**, 3641–3645.
37 H. Lee, Z. Yang, Y. Wi, T. W. Kim, P. Verwilst, Y. H. Lee, G.-i. Han, C. Kang and J. S. Kim, *Bioconjugate Chem.*, 2015, **26**, 2474–2480.
38 L. Yu, J. F. Zhang, M. Li, D. Jiang, Y. Zhou, P. Verwilst and J. S. Kim, *Chem. Commun.*, 2020, **56**, 6684–6687.
39 A. Heifetz, R. W. Keenan and A. D. Elbein, *Biochemistry*, 1979, **18**, 2186–2192.
40 M. Rocha, N. Apostolova, R. Diaz-Rua, J. Muntane and V. M. Victor, *Trends Endocrinol. Metab.*, 2020, **31**, 725–741.
41 M. Bhardwaj, N. M. Leli, C. Koumenis and R. K. Amaravadi, *Semin. Cancer Biol.*, 2020, **66**, 116–128.
42 S. Song, J. Tan, Y. Miao and Q. Zhang, *J. Cell. Physiol.*, 2018, **233**, 3867–3874.
43 N. Mizushima, T. Yoshimori and B. Levine, *Cell*, 2010, **140**, 313–326.
44 J. Mejlvang, H. Olsvik, S. Svenning, J.-A. Bruun, Y. P. Abudu, K. B. Larsen, A. Brech, T. E. Hansen, H. Brenne, T. Hansen, H. Stenmark and T. Johansen, *J. Cell Biol.*, 2018, **217**, 3640–3655.
45 I. Tanida, T. Ueno and E. Kominami, in *Autophagosome and Phagosome*, ed. V. Deretic, Humana Press, USA, 2008, vol. 445, ch. 4, pp. 77–88.
46 Y. Kabeya, N. Mizushima, T. Ueno, A. Yamamoto, T. Kirisako, T. Noda, E. Kominami, Y. Ohsumi and T. Yoshimori, *EMBO J.*, 2000, **19**, 5720–5728.
47 N. Mizushima, *Int. J. Biochem. Cell Biol.*, 2004, **36**, 2491–2502.
48 J. Guan, J. Sun, F. Sun, B. Lou, D. Zhang, V. Mashayekhi, N. Sadeghi, G. Storm, E. Mastrobattista and Z. He, *Nanoscale*, 2017, **9**, 9190–9201.